Skempton A. W. & Vaughan P. R. (1993). *Géotechnique* **43**, No. 1, 151–173

The failure of Carsington Dam

A. W. SKEMPTON* and P. R. VAUGHAN*

The upstream slope of Carsington Dam failed just before its completion in 1984. The slip started on the right abutment and spread across the valley to a length of nearly 500 m. Extensive investigations were conducted, and further information was obtained when the dam was reconstructed. The initial slip sheared through the core, which contained shear surfaces due to rutting, and along a layer of Yellow Clay which contained solifluction shears. Both materials were brittle, with low residual strengths. The factor of safety based on measured peak strengths was about 1·4; with reductions to allow for shears it was 1·2. It had been reduced to 1·0 by progressive failure. Finite element (FE) analyses in which strain-softening was reproduced confirmed this. It was concluded that the slide spread by lateral load transfer, through sections of the dam with a safety factor greater than 1. In the valley centre, the slide passed through the base of the mudstone fill. A combination of FE and limit equilibrium analysis indicated that the factor of safety just before collapse was about 1·1. The factor of safety was 1·6 with intact strengths and 1·4 after allowance for shears. The reduction to 1·1 was due to progressive failure; from 1·1 to 1·0 it was due to lateral load transfer.

KEYWORDS: case history; dams; embankments.

La pente amont du barrage de Carsington s'est écroulée en 1984 juste avant son achèvement. Le glissement a commencé sur le contrefort droit et s'est propagé au travers de la vallée sur une longueur d'environ 500 m. Des études approfondies ont été menées et des informations complémentaires ont été obtenues lors de la reconstruction du barrage. Le glissement initial s'est propagé par cisaillement au travers du noyau, où l'on observe des surfaces de cisaillement dues à des stries, ainsi qui le long d'une couche d'argile jaune qui présente des cisaillements de solifluxion. Les deux matériaux présentaient des comportements fragiles, à faibles résistances résiduelles. Le facteur de sécurité, calculé à partir des contraintes maximales mesurées, était égal à environ 1,4. Il a été réduit à 1,2 en raison du cisaillement, puis à 1,0 par suite de la rupture progressive. Une analyse par éléments finis, reproduisant la relaxation des déformations, confirme ces résultats. Il apparaît qui le glissement s'est propagé par transfert latéral de la charge à travers des sections du barrage à facteur de sécurité supérieur à 1,0. Au centre de la vallée, le glissement a traversé la base du remblai de mudstone. Les analyses par élément finis combinées aux analyses par équilibres limites montrent que le facteur de sécurité était de l'ordre de 1,1 juste avant la rupture. Il était égal à 1,6 pour les contraintes originelles et à 1,4 lors de l'apparition du cisaillement. La réduction jusqu'à 1,1 est due à la rupture progressive; De 1,1 à 1,0, elle est due au transfert latéral de la charge.

Paper to be presented at a meeting of the Institution of Civil Engineers at 3.00 p.m. on 27 April 1993 together with papers Carsington Reservoir—reconstruction of the dam, by J. K. Banyard, R. E. Coxon and T. A. Johnston (*Proc. Instn Civ. Engrs Civ. Engng*, 1992, **92**, Aug., 106–115), Reconstructed Carsington Dam: construction, by A. Macdonald, G. M. Dawson and D. C. Coleshill (*Proc. Instn Civ. Engrs Wat. Marit. & Energy*, 1993, **101**, Mar., 17–30), and Reconstructed Carsington Dam: design and performance, by R. W. Chalmers, P. R. Vaughan and D. J. Coats (*Proc. Instn Civ. Engrs Wat. Marit. & Energy*, 1993, **101**, Mar., 1–16).
Discussion on this Paper closes 1 July 1993; for further details see p. ii.

* Imperial College of Science, Technology and Medicine, London.

INTRODUCTION

A typical section of the Carsington dam as designed and a plan of the works are shown in Figs 1 and 2. Intended crest level was el. 202, 37 m above the stream bed. The dam had a clay core with an upstream extension (the 'boot'), and shoulders of compacted mudstone with drainage layers of crushed limestone about 4 m apart. Fill placing began in May 1982 and took three summers, with winter shutdowns from October to April at bank level el. 182 in 1982–83 and at el. 197–198 in 1983–84. A small berm was placed at the upstream toe as compensation for an increased rate of construction in August 1983.

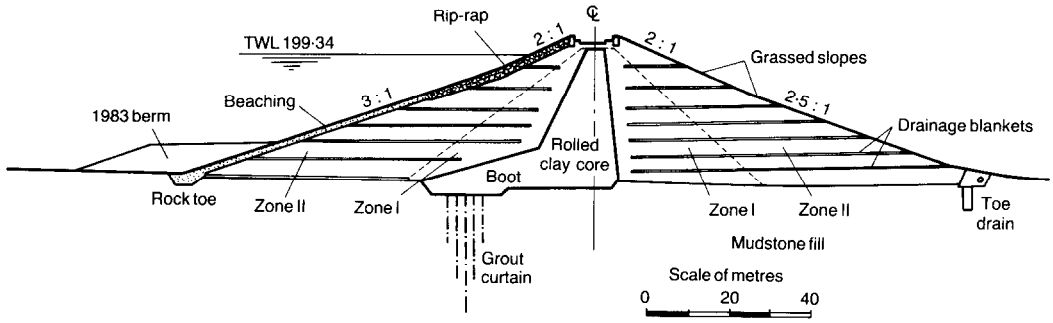

Fig. 1. Typical section of dam

Filling recommenced in May 1984, and on 1 June, the fill had reached el. 200–201, the level at which failure occurred.

Observations of pore pressures and settlements were made throughout construction at four instrumented sections, and horizontal displacements of pegs on the upstream face were observed from August 1983. Measurements were continued during the failure, which began early in the morning of 4 June 1984, over a length of about 120 m centred on ch. 725 on the north flank of the valley, where the bank was about 1 m short of its final crest level. The slip propagated along the embankment in both directions, extending finally to a length of nearly 500 m, with very large settlements of the crest and matching outward movements of the upstream toe.

Babtie Shaw & Morton and Professor A. W. Skempton were commissioned by the owners to establish the cause of the failure. Details of the investigation are given by Rocke (1993). Work on site was completed by the end of September 1984, but laboratory testing continued for several months afterwards. Babtie Shaw & Morton and Professor Skempton submitted an interim report in October 1984, and a report on the principal findings of the investigations in March 1985. Accounts of the failure were published at this time (Skempton & Coats, 1985; Skempton, 1985). A final report was submitted in April 1986. The findings of this report were summarized by Coxon (1986).

The present Paper is essentially a summary of the 1986 final report, with some modifications based on further tests and on observations made during dismantling of the original dam and construction of its replacement, and on additional information from further finite element (FE)

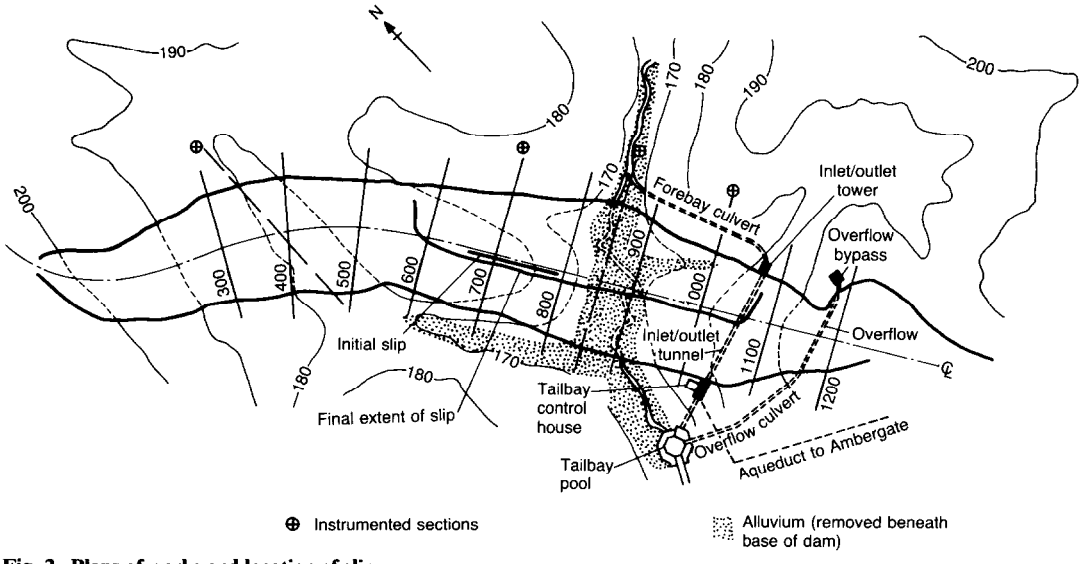

Fig. 2. Plans of works and location of slip

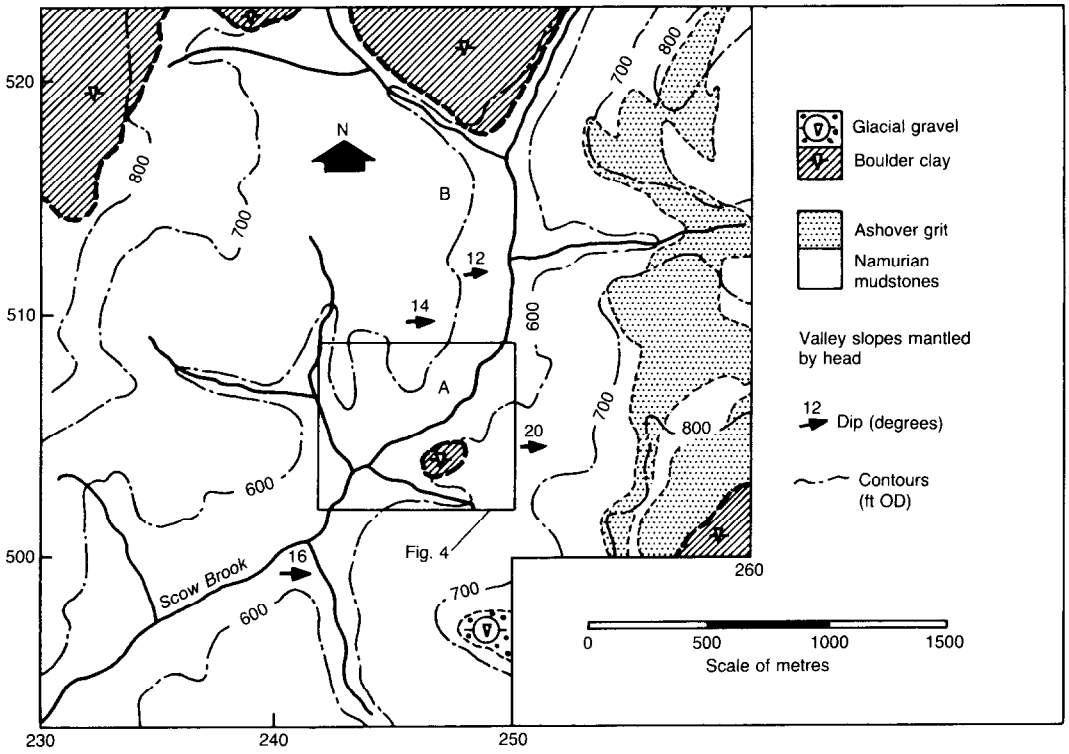

Fig. 3. Geology

analyses performed at Imperial College (Dounias, 1987; Dounias, Potts & Vaughan, 1989; Potts, Dounias & Vaughan, 1990). The failure has been discussed extensively, and the principal technical contributions are listed in the references and bibliography.

GEOLOGY

The dam is six miles north-east of Ashbourne in Derbyshire. It crosses a broad valley with a central flood plain 50–80 m wide. Bedrock is Upper Carboniferous (Namurian) mudstone with occasional thin bands of sandstone. Boulder clay

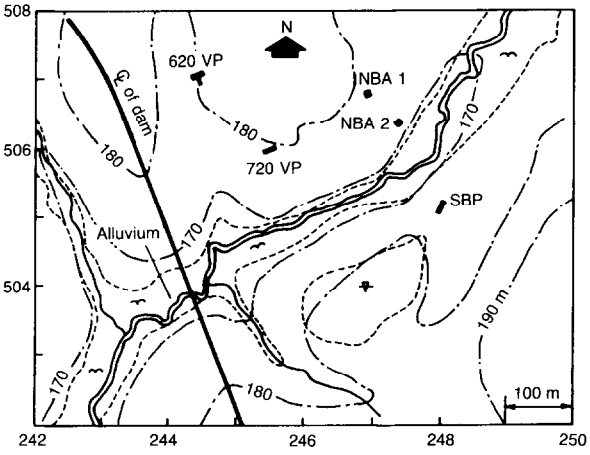

Fig. 4. Location of trial pits

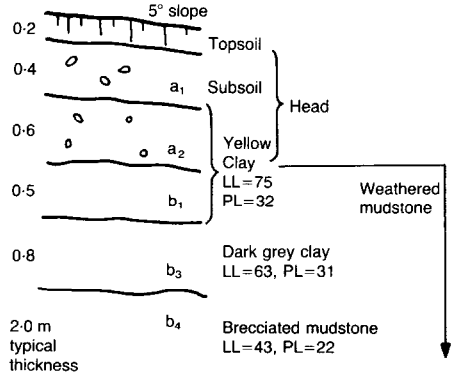

Fig. 5. Geological profile in natural ground: shear surfaces found near junction of a_2 and b_1

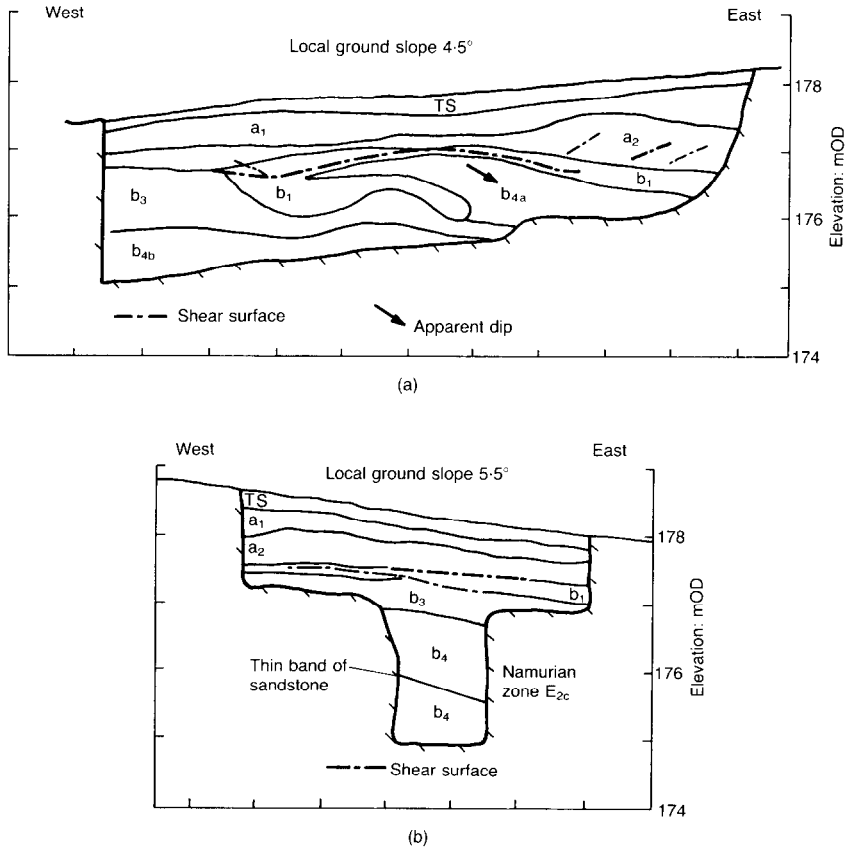

Fig. 6. Sections of pits showing solifluction shears: (a) trial pit 620VP, north face; (b) trial pit NBA1

and patches of glacial gravel exist on the neighbouring higher ground, and in places boulder clay survives on the valley sides (Fig. 3). The site lies well outside the limits of the last (Devensian) glaciation, so the glacial deposits belong to the Older Drift, and are probably of Wolstonian age.

Four trial pits were excavated as part of the investigation of the site in the north flank of the valley in area *A* (Fig. 4). Together with borings in area *B* (Fig. 3), they show that the lower parts of the slopes, inclined at 4°–6°, are mantled by a layer of head averaging 1·2 m in thickness. On the steeper slopes (8°–9°) on the opposite (south) side of the valley the head is slightly less thick. A typical section (Fig. 5) shows head consisting of silty clay subsoil a_1 and plastic yellow-brown clay a_2, both containing scattered sandstone fragments and rare quartz pebbles derived from the glacial deposits, overlying a layer of completely weathered mudstone b_1 almost identical to soil a_2 except that it has no foreign inclusions. For geotechnical purposes a_2 and b_1 can be grouped together as 'Yellow Clay'. Below this the mudstone is usually dark grey, with some red-brown mottling, and changes with depth from clay b_3 to a brecciated material b_4 and then to a weak mudstone b_5 consisting of lumps or blocks in a stiff clay matrix. Finally, at a depth of 10–15 m, unweathered mudstone b_6 is encountered, heavily jointed with bedding planes dipping at about 15° to the east. In the flood plain, alluvium consisting

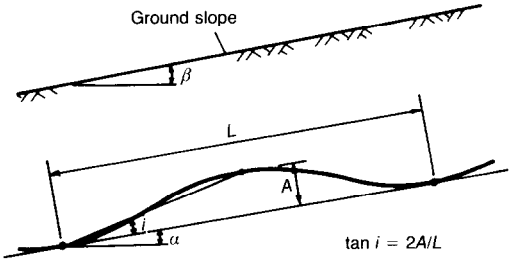

Fig. 7. Idealized undulation in shear surface

Table 1. Properties of foundation strata

Property		Yellow Clay (a_2 and b_1)	Grey clay (b_3)	Brecciated mudstone (b_4)	Mudstone (b_5)
Water content w: %		38	27	18	14*
Liquid limit w_L: %		75	63	43	44
Plastic limit w_p: %		32	31	22	23
Plasticity index (PI): %		43	32	21	21
Clay fraction (CF): %		62	47	32	33
Activity (PI/CF)		0·69	0·68	0·65	0·64
Peak strength (intact)	c_p': kPa	10	15	15	18*
	Φ_p'	20°	22°	24°	27°*
Residual strength	c_R': kPa	0			
	Φ_R'	12°			

* Recompacted, fresh from borrow pit.

of soft sandy clay over a thin basal bed of clayey gravel replaces the weathered mudstone down to b_4 or b_5.

Mudstones b_5 and b_6 contain inclusions of pyrites. On exposure to air this oxidizes to release sulphuric acid, which liberates iron, calcium and other elements into solution with consequent softening or partial disintegration of relatively hard 'fresh' mudstone. The chemical changes were illustrated by the accumulation of pools of acidic iron-stained water on freshly exposed mudstone in the fill or borrow pits, and by the generation of CO_2 gas from the acid reaction with the calcium carbonate in the mudstone and the limestone drainage blankets in the dam. They also play a part in the much slower weathering process in situ, which has reached completion with the elimination of pyrites in the layers down to and including b_4, although layers up to b_1 remain acidic.

At many sections in the borrow pits, particularly in area B (Fig. 3), and in the foundation below the dam, severe folding was seen in the beds above b_6, amounting in places to sharp angular folds, the result of periglacial cryoturbation, involving the growth and decay of ground ice. All signs of bedding and superficial folding disappear in the Yellow Clay; instead there are discontinuous shear surfaces lying subparallel to the ground slope. These are smooth but not polished, and gleyed, and were caused by down-slope movement due to freezing and thawing during solifluction in the Devensian period.

Table 2. Properties of fill materials

Property		Core	Zone I	Zone II
Standard compaction	w_{opt}: %	26	20	14
	γ_d: kN/m^3	14·6	16·2	18·1
In situ properties	w: %	34	24	14, 18*
	γ_d: kN/m^3	13·6	15·4	18·3
Liquid limit w_L: %		69	56†	45
Plastic limit w_p: %		31	29	23
Plasticity index (PI): %		38	27	22
Clay fraction (CF): %		56		34
Activity (PI/CF)		0·68		0·65
Specific gravity G		2·68	2·71	2·71
Peak strength	c_p': kPa	15	10	17
	Φ_p'	21°	22°	26°
Residual strength	c_R': kPa	0		0*
	Φ_R'	13°		15°*

* From shear zone (small samples).
† Single test only.

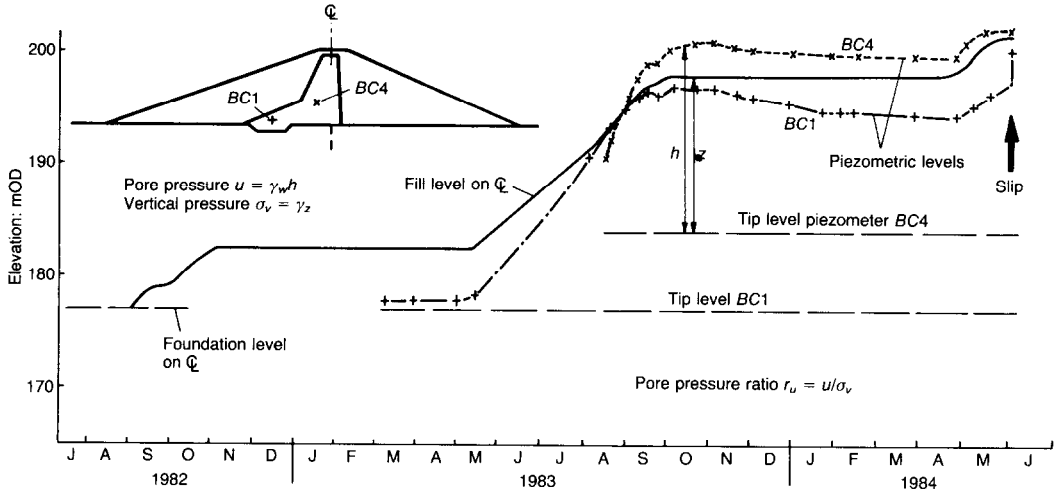

Fig. 8. Typical piezometer records from core and boot at ch. 705

Solifluction shears occurred over 40% of the total length (56 m) examined in pits on the north side of the valley where the slope is around 5°. Two examples are shown in Fig. 6. The undulations in the shear surfaces in this area can be quantified approximately by an angle $i = 3°$ as sketched (to an exaggerated vertical scale) in Fig. 7. On the south side of the valley, with a ground slope of 8°, the shears were flatter and more extensive. Details of the exploratory pits, and an illustration of the soil fabric in thin section, which shows substantial alignment of particles along a shear surface, are given by Skempton *et al.* (1988).

Index properties of the strata are summarized in Table 1. They reveal a marked increase in water content, plasticity and clay fraction with degree of weathering. In the dam (Fig. 1), the following three zones of fill were used, with index properties as summarized in Table 2.

(*a*) The central core and the boot, formed of material from the a_2, b_1 and b_3 strata, compacted at natural water content (average $w = 34$), 8 percentage points above the average optimum water content from the standard compaction test (26).
(*b*) The outer shoulders, formed from b_5 strata, referred to as zone II fill. Average water content was 16, close to optimum.
(*c*) Transition zones either side of the core, referred to as zone I fill, formed mainly from b_3 and b_4 strata, with an average water content ($w = 20$) 4 percentage points above optimum (16).

Rip-rap slope protection and a stone upstream toe of Derbyshire limestone rockfill, and drainage layers of crushed limestone, were also used.

In the valley centre the alluvium and some of the basal gravel were removed, and the dam was founded on weathered b_4 or b_5 mudstone. On the valley sides the shoulder and central core were founded on Yellow Clay, only topsoil and subsoil being removed. The boot was founded at slightly greater depth, with a grout curtain below.

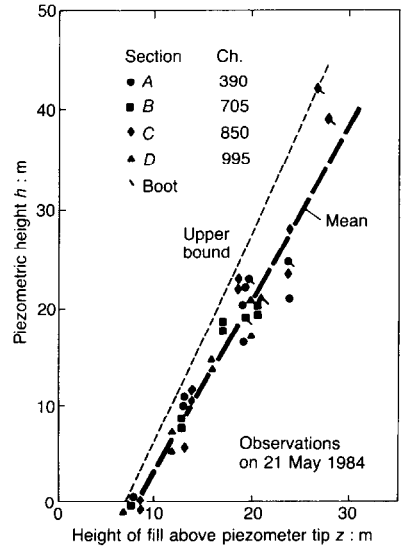

Fig. 9. Relationship of pore pressure in core and boot and depth of fill immediately before collapse

OBSERVATIONS OF PERFORMANCE BEFORE FAILURE

Pore pressure

Typical pore pressures measured in the core and boot are plotted in Fig. 8, and the last complete set of readings before the failure, taken on 21 May, are plotted against height of fill in Fig. 9. The upper bound shown represents an increase in pore pressure equal to the increase in nominal overburden pressure. The original (negative) pore pressures become zero under 7 or 8 m of fill.

Pore pressures in the zone I fill become positive only under 12 m of fill. They averaged about 5 m of water head under 20 m of fill, higher pore pressures being observed in the fill below the winter shutdown surface of 1982–83, where the fill had become wetter. No excess construction pore pressures were observed in zone II fill, or in the foundation strata; pressures up to 21 May corresponded to ground water levels of el. 170 m in the valley centre and near the base of the Yellow Clay at ch. 705.

Vertical compression in the fill

Compressions between the plates of vertical settlement gauges in the core 4 m upstream of the centreline are plotted against elevation in Fig. 10(a) for the end of the 1983 placing season. They are large but unremarkable, except for the compression at a depth of about 20 m at ch. 850 m, which increased from 7% to 9% by the end of October, when the access tube to the gauge became blocked. This depth corresponds to the eventual failure surface, and to the point of maximum deviatoric strain (15%) predicted by the FE analysis for this section with the fill at el. 197·5 m, although at this stage there were still quite small strains along the base of the mudstone fill, where failure subsequently occurred.

The instrumented section at ch. 705 is within the length of the initial slip. Ten days before failure, with bank level at el. 200, measured vertical compression reached a maximum of about 6%. By 1 June 1 m of fill had been added, and vertical compression at a depth of 14 m had increased to 11%. This corresponds to the location of the eventual failure surface.

Upstream peg displacements

Observations of the lower line of pegs began on 18 August 1983 with the bank level at el. 193. Displacements at ch. 750 and ch. 875, representative of displacements at what became the initial slip and at the valley centre, are plotted against time in Fig. 11, with starting points matched to displacements predicted by FE analyses at nearby sections (ch. 725 and ch. 850). At ch. 750 observed movements are similar in magnitude to those predicted by analysis up to 1 June 1984, and the fill elevation at failure predicted by the analysis almost coincides with that observed. At ch. 875 movements predicted by a matching FE analysis are larger than those measured, probably due to shortcomings in the modelling of the stiffness of

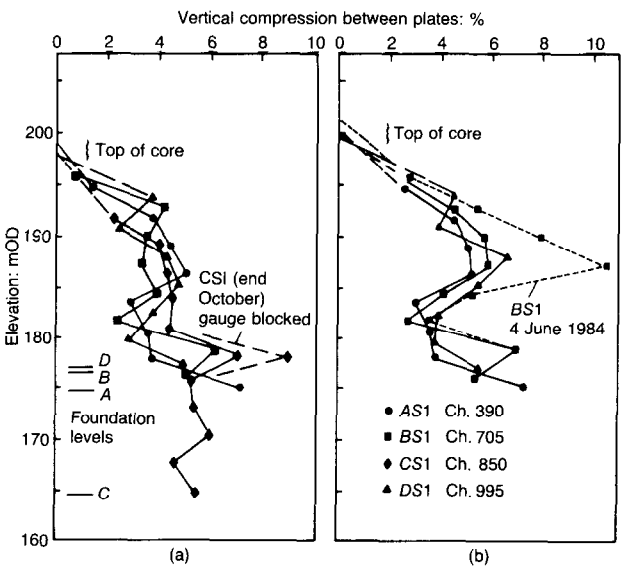

Fig. 10. Vertical strain measured by USBR settlement gauges in core 4 m upstream of centreline: (a) October 1983; (b) 24 May 1984

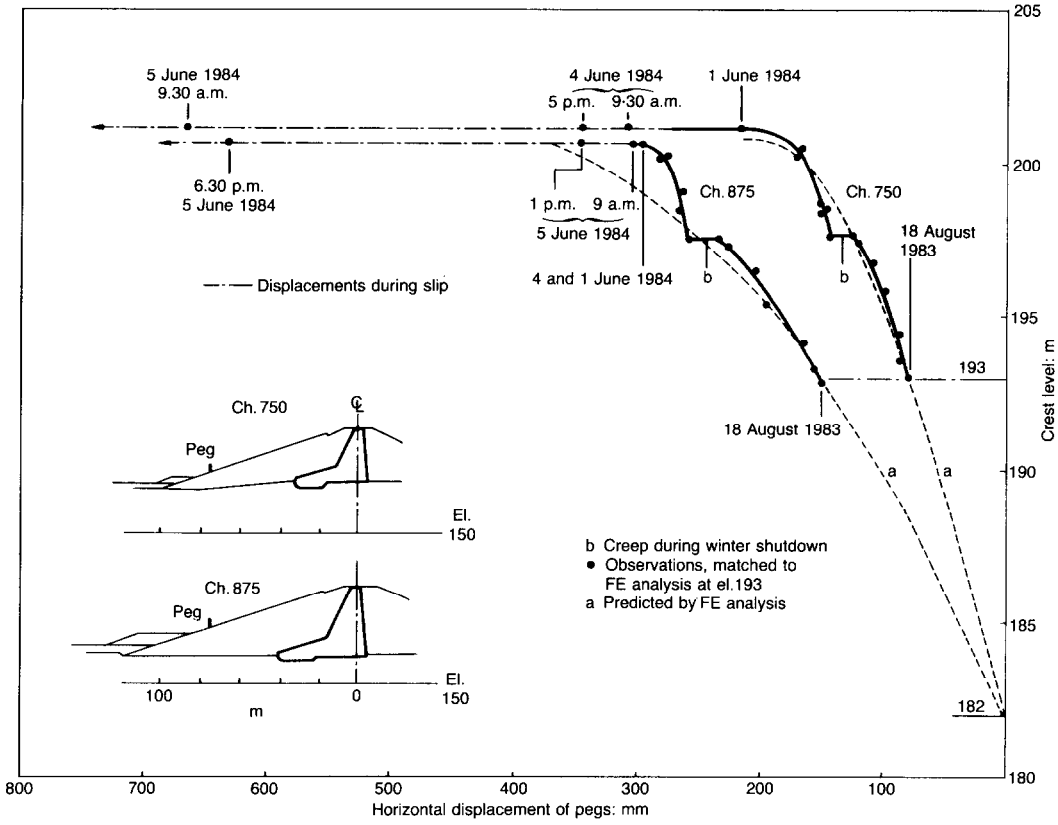

Fig. 11. Measured horizontal movements at toe pegs, and predictions of these movements from the FE analyses

the fill in the finite element analysis (Potts *et al.*, 1990).

A feature of the peg movements is the creep observed during the 1983/4 winter shutdown, particularly at ch. 875, and the subsequent increased 'stiffness' when construction restarted. Note also the disproportionate increase in displacement at ch. 750 (nearly 50 mm) between 25 May and 1 June, as only 0·8 m of fill was placed. Up to that point the larger movements at ch. 875 than at ch. 750 reflect the difference in height of fill above foundation level (35 m and 28 m respectively at final level). The maximum difference in displacement at the two sections before the initial failure was 110 mm and, as the sections are 125 m apart, the average longitudinal strain along the embankment never exceeded 0·1%. Displacements and strains within the embankment might be twice as much, but an analysis of lateral load transfer (Vaughan, 1991) has shown that such strains do not allow significant transfer of load along the embankment.

THE FAILURE

The toe pegs were surveyed in the afternoon of Friday 1 June 1984. No fill was placed during the weekend, which was wet. When the workforce arrived on site at 7.30 a.m. on Monday 4 June, a tension crack was seen on the crest from about ch. 670 to ch. 790. A survey of the pegs at 9.30 a.m. showed that additional movements of 75 mm and 95 mm had occurred at ch. 675 and ch. 750 since Friday. Evidently a slip was developing in the upstream slope; construction of an emergency toe berm from ch. 675 to ch. 750 started in the afternoon.

The development of movement during the failure is shown in Fig. 12. By 2.00 p.m. the crack extended from ch. 655 to ch. 830, and had a maximum width of about 50 mm. By 5.00 p.m. the pegs at ch. 675 and ch. 750 had moved a further 40 mm at an average rate of 6 mm/h, and were moving at about 10 mm/h. Meanwhile no movement was measurable at the peg at ch. 875.

By 9.30 a.m. Tuesday 5 June, peg movements

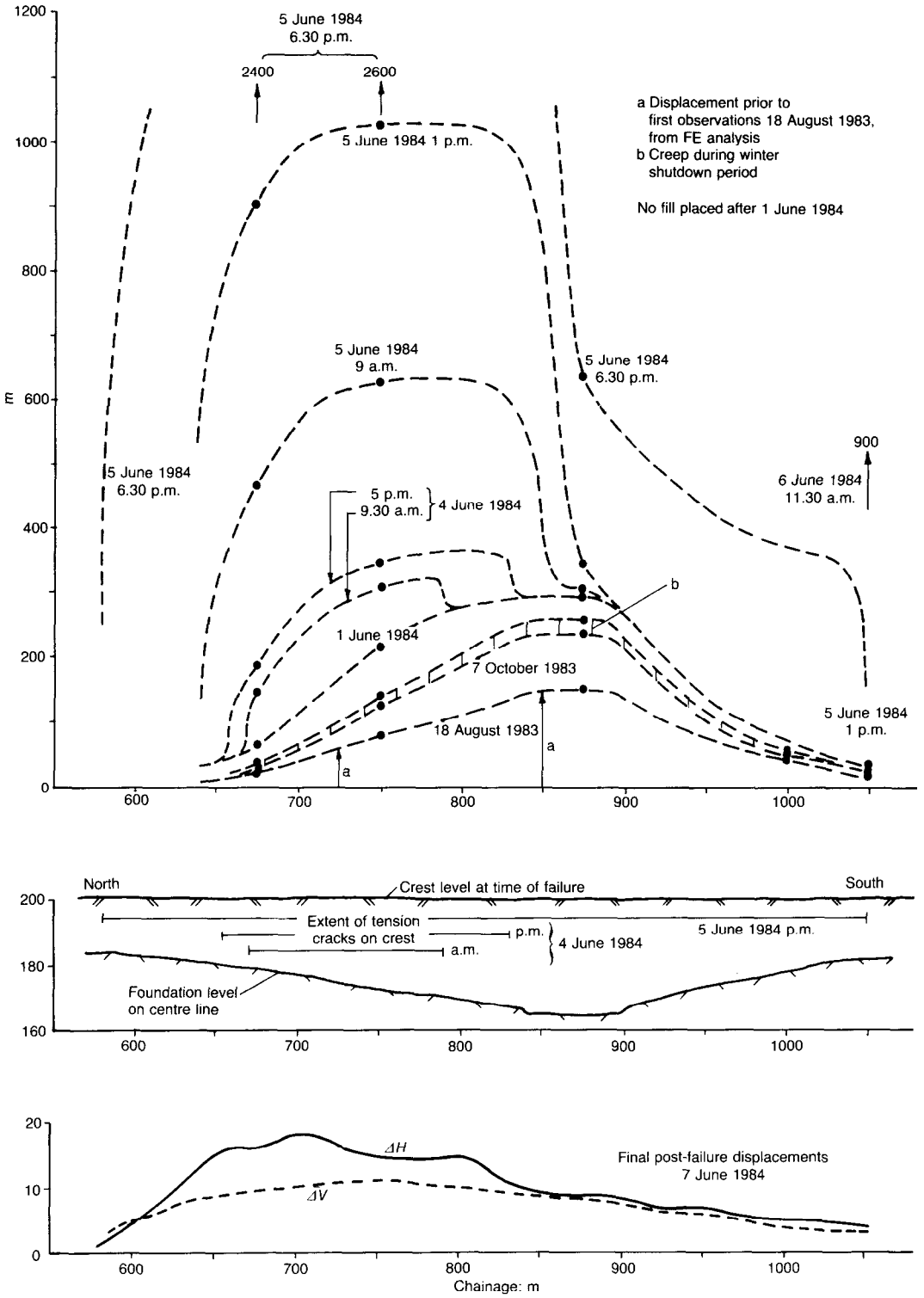

Fig. 12. Horizontal displacement before, during and after the slip

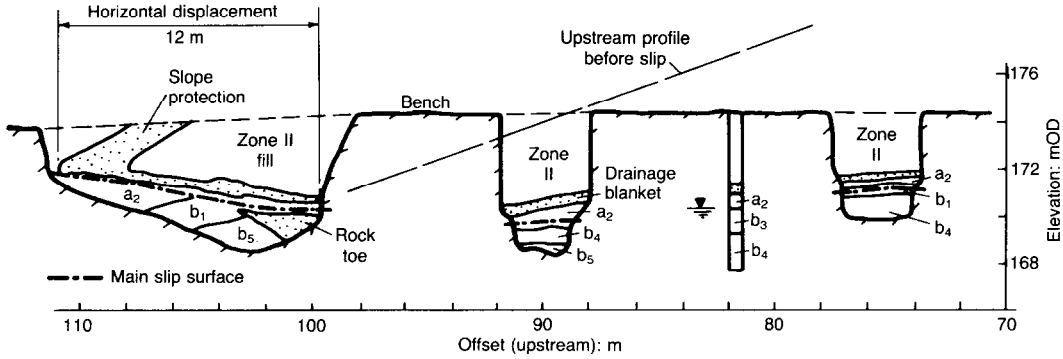

Fig. 13. Sections of trial pits showing slip surface at ch. 720

were nearly 300 mm at ch. 675 and ch. 750, where the crack was up to 350 mm wide and the crest had slumped about the same distance. For the first time a small additional horizontal displacement (not more than 10 mm) was observed at the toe peg at ch. 875. This displacement became 45 mm by 1.00 p.m. A second crack had appeared about 2 m downstream of the first one between ch. 670 and ch. 750, and around noon a graben depression began to form in this area. By late afternoon cracking extended from ch. 580 to ch. 1050, and the movement of the pegs was about 2·5 m over the length of the initial movement and 0·6 m in the valley centre.

Large movements occurred overnight, and by the morning of Wednesday 6 June maximum horizontal movement was 13 m, with crest settlement approaching 10 m. The slip had extended to its final length from ch. 580 to ch. 1075. Movement ceased by Thursday 7 June. The final horizontal movement of the upstream face and the crest settlement are shown in Fig. 12. Propagation of the failure along the embankment was associated with average longitudinal shear strains between pegs of the order of 1%.

EXPLORATION OF THE SLIP

Open trenches were excavated into the toe of the slip at ch. 620, ch. 720 (the initial failure) and ch. 825 (the highest section), from which timbered pits were sunk to examine slip surfaces and other features. Borings and cone penetrometer profiles were made at ch. 720 and ch. 825 to determine the position of the displaced drainage layers and the upstream boundary of the core.

At ch. 720 the two pits showed two closely spaced slip surfaces (a single entity in Fig. 13) with several minor shears in the Yellow Clay (a_2 and b_1) beneath the basal drainage layer. The main shears were seen to be polished and striated in the direction of slip movement. They were at a similar depth within the profile to the solifluction shears observed outside the slip. Through the core the location of the slip surface was indicated approximately by the breakage of tubes to piezometers within the slip at the instrumented section at ch. 705, and the survival of those outside. Various points within the slip and on the slope could be identified before and after movement, enabling displacement vectors to be constructed, as in Fig. 14(a). A reasonably accurate picture of the total slip movement was thus constructed.

At ch. 825, in the valley centre (Fig. 15) the main slip surface and an associated secondary shear were located in zone II fill about 1 m above the basal drainage layer, and in places shear zones existed immediately adjacent to these slip surfaces. In addition, on one side of the inner pit, a shear surface was seen just above the drain layer in the first layer of fill, which contained some mottled clay and gravel as well as mudstone (not typical of zone II). These shear surfaces were striated and polished. In the side of the trench, about 3–4 m above the main slip, a horizontal discontinuity was found several metres long, smooth but only locally striated. It may have been formed by slight movement on a weak surface between fill layers. The slip movement, estimated as for ch. 725, is shown in Fig. 14(b).

In the pit at ch. 620 the main slip surface passed through Yellow Clay (a_2) below the basal drain layer, cutting through the blanket to pass over the stone toe, with an overthrust of 6 m as shown in Fig. 16. Like the other main shears, this was polished and striated in the direction of the slip, and was associated with shear zones and secondary shears. One of the latter continued below the basal drain layer where this remained in place near the toe, but the polish and striations died away towards the rock toe, consistent with a small and decreasing displacement. Another slip surface was observed in the zone II fill. This was consistently 300 mm above the disrupted drain-

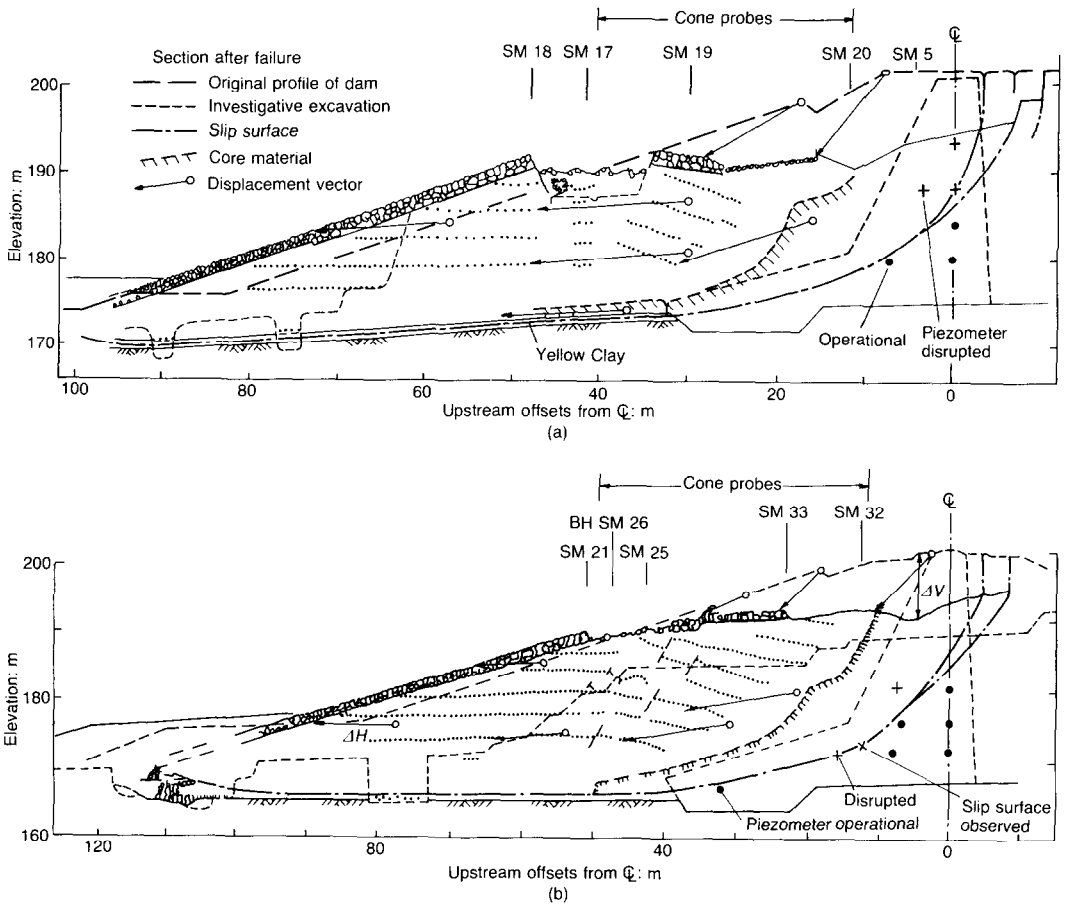

Fig. 14. Reconstruction of slip movement: (a) at the initial failure (ch. 720); (b) in the valley centre (ch. 825)

age layer, as if following the surface of the bottom layer of fill. It joined the main slip surface at the overthrust, and had clearly moved during the slip, although by an unknown amount. The FE analyses indicate that this part of the slip would have formed quickly after collapse had started as the slip 'ran away'. Failure in the Yellow Clay would have been undrained. At the low normal effective stresses operating in this location the Yellow Clay would have been dilatant, with an undrained strength greater than its drained strength, and possibly greater than the peak strength of the partly saturated mudstone fill above. This observation indicates that the two

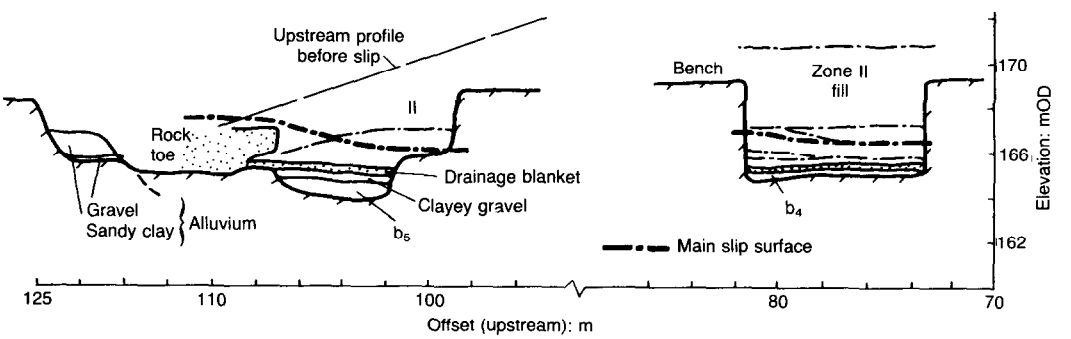

Fig. 15. Sections of trial pits showing slip surface at ch. 825

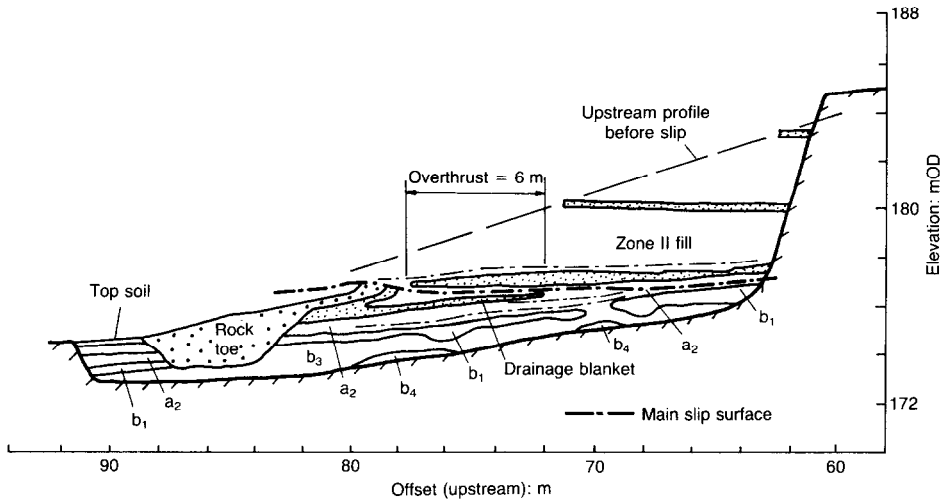

Fig. 16. Section of trial pit showing slip surface at ch. 620

materials must have had comparable strengths at this location. No other example of slip surfaces in both the foundation and the fill was noticed during removal of the dam, but this could have occurred locally.

The location of the slip surface as observed during removal of the dam in 1989 is shown in Fig. 17. Its location in the Yellow Clay on both flanks of the valley, and in the zone I and zone II fill in the valley centre was confirmed. The 1984 trial pit at ch. 820 was found to be close to the boundary between the two types of movement, which may have influenced the formation of the sliding surface at this point. In the bottom of the valley where no Yellow Clay was present between ch. 970 and ch. 1040 and at ch. 880, part of the surface passed through a layer of remoulded clay a few millimetres thick on the foundation surface just below the basal drainage layer. This layer was probably caused by proof rolling of the foundation during construction. Most of this part of the failure surface would have formed at a late stage of the slip, and would have had little influence on failure. In the core several parallel shear surfaces were often seen. In the boot a single surface was usually seen.

In the zone II fill in the valley centre there were usually two or three slip surfaces between 0·5 m and 1·5 m above the basal drainage layer. These varied in level longitudinally, and did not appear to be following surfaces between compacted layers. In addition to these slip surfaces, other horizontal surfaces were seen within both the upstream and the downstream fill. Typically,

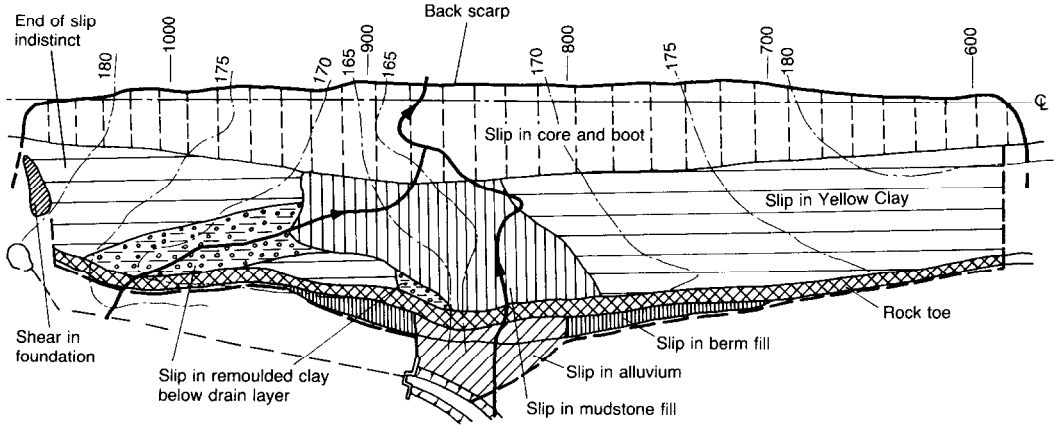

Fig. 17. Location of slip surface as surveyed during excavation of embankment

these were ~3 m in extent. They did not show polishing or striations indicating shear. The formation of sheared surfaces on the interface between a layer being compacted and the layer below has been recognized (White & Vakalis, 1983, 1985, 1987). No sheared surfaces were observed in the mudstone fill at Carsington, except in close proximity to the main slip surface. An alternative cause of shears within clayey fills is bearing capacity failure (rutting) under plant wheels. Such surfaces are curved and not horizontal. They were generated in the weak clay core, but were never seen in the zone II fill, which was much stronger, and were rarely seen in the zone I fill.

During the removal of the dam, solifluction shear surfaces were observed in the Yellow Clay outside the slide area. In one very local area downstream, and in one area at the south end of the slide (Fig. 17) shear surfaces were seen on bedding planes in the foundation. The second surface was about 10 m by 20 m, in planar bedding dipping into the dam abutment. It crossed grout holes used for consolidation around the tunnel, and dislocation of these showed that movement had not exceeded 70 mm. The cryoturbation of the mudstone in the top of the foundation had disrupted the bedding elsewhere, which prevented any general failure along bedding planes which might otherwise have occurred.

SHEAR STRENGTH OF MATERIALS IN AND BELOW THE SLIDE

Shear strength of foundation materials

Yellow Clay. Drained triaxial tests, direct shear tests and simple shear tests were carried out on intact samples. The peak strength parameters obtained (Fig. 18) were $c_p' = 10$ kPa, $\Phi_p' = 20°$. Stress–displacement curves from 300 × 300 × 150 mm and 60 × 60 × 20 mm direct shear box samples showed no significant scale effect. Direct shear box and triaxial tests were also conducted to measure the drained strength on samples containing the shear surface from the slip and on samples containing solifluction shears (Fig. 19). Both showed a drained residual strength of $c_R' = 0$, $\Phi_R' = 12°$. The reduced peak strength and the small displacement to residual (Fig. 19(b)) on the solifluction shears are typical. The shears concentrate strain so that particle orientation, polishing and the development of residual strength occurs in a few millimetres displacement, at an equivalent strain much less than is required to develop peak strength in intact samples. (Fig. 20). Thus if soil which contains a discontinuous shear surface is sheared along the plane of the surface, the surface will have reached residual strength before

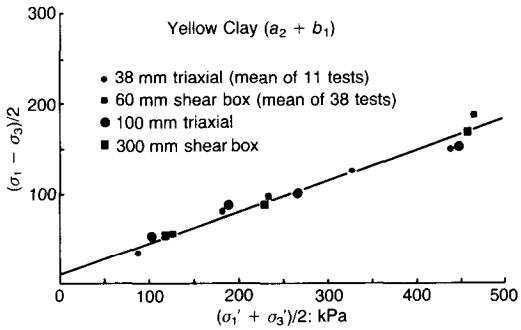

Fig. 18. Yellow Clay: peak intact drained shear strength ($w = 38$, $c' = 10$ kPa, $\phi' = 20°$)

the intact soil on either side has reached peak. To a reasonable approximation, the total peak resistance is given by the area of shear surface multiplied by its residual strength, plus the area of intact soil multiplied by its peak strength.

When shear surfaces undulate (Fig. 7) in the direction of sliding, as was the case at Carsington, the strength is increased. With an equivalent angle of dilation i less than ~4°, the residual shearing resistance on the surface c_s', Φ_s', is given (Dounias, Potts & Vaughan, 1988) by

$$c_s' = 0; \Phi_s' = \Phi_R' + i \quad (1)$$

With $i = 3°$, the value measured at Carsington, $\Phi_s' = 15°$.

The site investigation showed that the solifluction shears occupied 40% of the area of the Yellow Clay. Combining the effects of partial area and undulations described above gives the average peak bulk drained strength for the Yellow Clay as

$$c_p' = 10 \times 0{\cdot}6 + 0 \times 0{\cdot}4 = 6 \text{ kPa} \quad (2a)$$

$$\tan \Phi_p' = \tan 20 \times 0{\cdot}6 + \tan (12 + 3) \times 0{\cdot}4$$

$$\Phi_p' = 18° \quad (2b)$$

Dark grey clay. Five drained tests on intact 100 mm dia. triaxial samples and 300 × 300 × 150 mm direct shear box samples gave average peak strength parameters of $c_p' = 15$ kPa; $\Phi_p' = 22°$.

Brecciated mudstone. Six drained tests on 100 mm dia. triaxial samples of intact mudstone gave average drained peak strength parameters of $c_p' = 15$ kPa, $\Phi_p' = 24°$. Two additional samples failed on bedding planes. The strength on these planes was $c_p' = 0$, $\Phi_p' = 18°$. Φ' decreased by ~2° with small displacements on the failure plane. Such bedding planes would have been potentially weaker than the Yellow Clay or the fill. However, as already described, the superficial folding in the dam foundation caused by periglacial cryoturbation prevented failure along such planes, except in the two locations described.

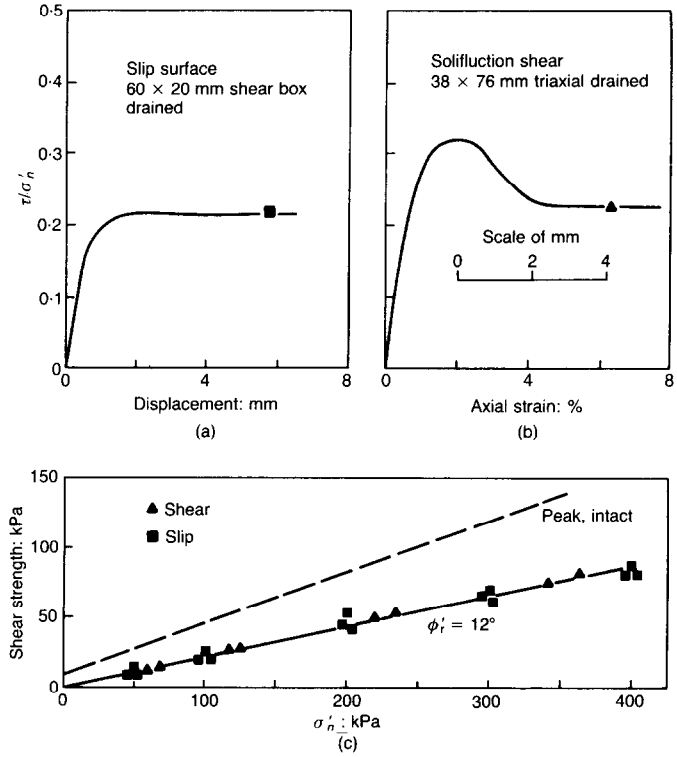

Fig. 19. Yellow Clay: drained shear strength on solifluction shears and slip surfaces

Shear strength of fill materials

Core. Peak (maximum stress ratio) strengths were measured in undrained triaxial tests with pore pressure measurement, at the sample base and by probe at mid-height, on 100 mm dia. samples. Peak strength was developed at ~3·5% axial strain. The average strength envelope was $c_p' = 15$ kPa; $\Phi_p' = 21°$. The strength on the shear surfaces in the core caused by rutting by construction plant were measured in 38 mm dia. drained triaxial samples. The average peak drained strength envelope for the shear surfaces was $c_{ps}' = 0$; $\Phi_{ps}' = 16°$. This strength was generated when the axial strain was typically 2·5%. The strength on the surface then dropped rapidly to $c_R' = 0$; $\Phi_R' = 13°$, reached at an axial strain in the sample of about 7%. Peak strength would therefore not be developed simultaneously in the intact clay and on the shear surfaces. It was thus thought reasonable to assume that the strength mobilized on the shear surfaces would be $c' = 0$, $\Phi_s' = 15°$ when the peak strength of the bulk soil was reached. Vaughan (1985) and Potts *et al.* (1990) have evaluated the effect of random shears in a mass of clay by considering a two-dimensional assembly of blocks in each of which a plane shear occurs at a random angle. The bulk strength of the mass of soil, $q^* = (\sigma_1 - \sigma_3)/2$, is the average strength of all the blocks and is given by

$$q^*/q_p = \{2\xi - \sin\xi \ln[(1 - \cos\xi)/(1 + \cos\Phi)]\}/\pi \quad (3)$$

where q_p is the shear strength at failure of the intact soil

$$q_p = c_{ip}' \cos\Phi_{ip}' + s' \sin\Phi_{ip}' \quad (4a)$$

$$s' = (\sigma_1' + \sigma_3')/2 \quad (4b)$$

$$\sin\xi = s' \sin\Phi_s'/q_p \quad (4c)$$

The strength on the discontinuity is $c_s' = 0$, $\Phi' = \Phi_s'$. Equation (3) gives a reasonable prediction of the bulk strength of fissured London clay (Sandroni, 1976). With $\Phi_s' = 15°$, $c_{ip}' = 15$ kPa, $\Phi_{ip}' = 21°$, the envelope for q^* becomes $c' = 6$ kPa; $\Phi' = 20°$.

Zone II fill. Drained tests on large samples of the fill taken in June–July 1984 gave a peak strength envelope (Fig. 21(a)) described by $c_p' = 17$ kPa, $\Phi_p' = 26°$. The water contents and dry densities of the test samples are plotted in Fig. 22. Drained direct shear box tests on the main slip

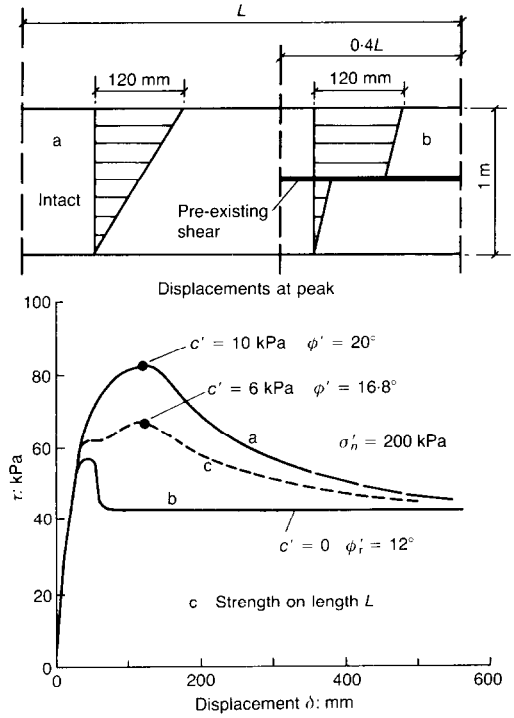

Fig. 20. Yellow Clay: composite stress/displacement curves for a layer containing a planar shear occupying 40% of its area

surface at ch. 825 and on the slip surface at ch. 620 (Figs 15 and 16) both gave $c_R' = 0$, $\Phi_R' = 15°$ (Fig. 21(b)).

Chemical changes occur when b_5 mudstone is oxidized: the samples of zone II fill were taken soon after the failure, about two years after the fill was placed, and should represent the fill as it was when the slide took place. Various tests done later on samples that were recompacted and thus broken down, and on in situ samples that had been subject to surface weathering, indicate that the drained strength varied consistently with the dry density of the fill tested, rather than with the amount of mechanical or chemical breakdown. About half the difference in water content between the general fill ($w = 14$) and the shear zone ($w = 18$) reflects the absence of mudstone 'lumps' in the small samples that were used for the shear zone tests. The remaining difference could be due to dilation in the shear zone. The small amount of data available from the initial investigation indicated that the density of the base of the fill was less than elsewhere; a small reduction in strength was assumed in the 1986 report to account for this. No evidence for this reduced density was found when the dam was removed, and this correction is no longer considered relevant.

As is discussed below, the behaviour of the slide in the valley centre where failure took place

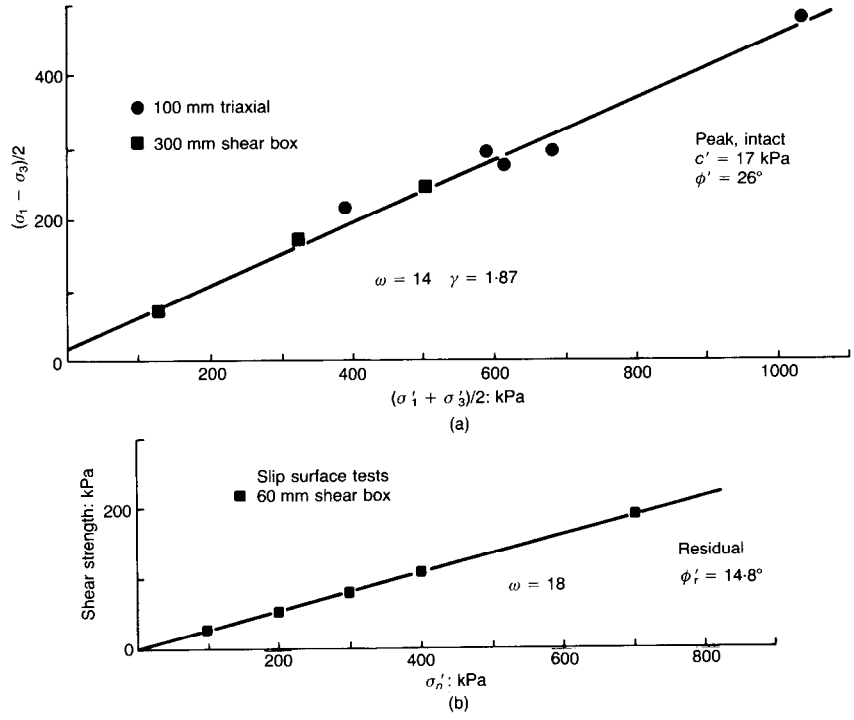

Fig. 21. Zone II fill drained shear strength: (a) main fill; (b) shear zone

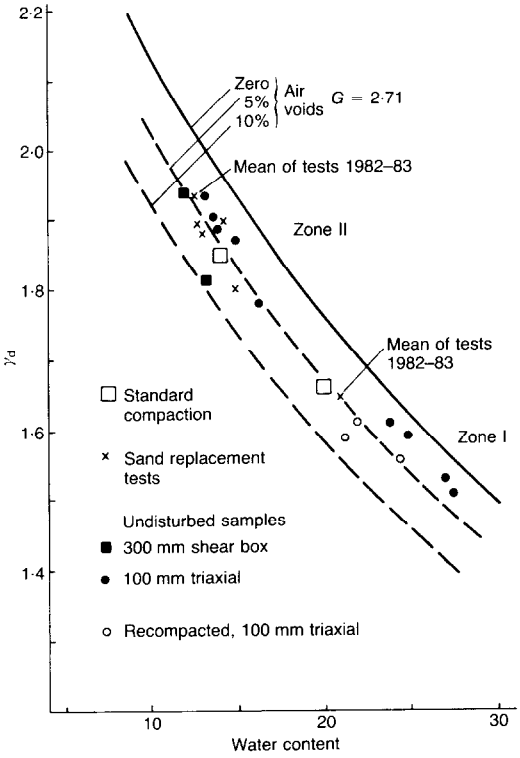

Fig. 22. Mudstone fill: compaction test results and in situ densities

through the zone II fill was consistent with a strength lower than was measured by laboratory triaxial tests on intact samples. The test samples were not large enough to reflect fully the effect of construction layers, and shearing in the tests was across them. Even when no discrete surface of separation between layers can be seen, as was generally the case at Carsington, some reduction of strength along the compacted layers can be expected on the grounds of reduced dilatancy of the fill at the interface, and orientation of the larger particles in the horizontal direction during compaction. Close inspection of the fill showed that the larger slab-like pieces of mudstone did lie mainly horizontally, and that the squeezing of the clay matrix against them during compaction had sometimes produced polishing on their surfaces. Such lumps were not present in test samples. Both layering and the polished blocks tend to create discontinuities in stress and strain and increase the rate at which strength is lost with post-peak movement.

The effect of this structure on peak strength can be allowed for. The peak strength on horizontal surfaces must lie between the peak intact strength measured in the laboratory and the residual strength, with the latter increased by an allowance for undulation of the surfaces. This may be taken as $c' = 0$, $\Phi' = 16°$ (conservatively estimated as residual strength plus $i = 1°$). A reduction of 20% from peak to residual then becomes

$$c_p' = 17 \times 0{\cdot}8 = 13{\cdot}5 \text{ kPa} \quad (5a)$$

$$\tan \phi_p' = \tan 16° + (\tan 26° - \tan 16°) \times 0{\cdot}8$$

$$\Phi_p' = 24° \quad (5b)$$

The effect of varying this reduction is examined below. A residual strength of $c_R' = 0$, $\Phi_R' = 14{\cdot}5°$ was adopted for the FE analysis.

Zone I fill. Undrained triaxial tests on four 100 mm dia. samples of the intact fill, and three samples recompacted at the same density, gave a consistent peak strength envelope described by

$$c_p' = 10 \text{ kPa}; \Phi_p' = 22° \quad (6)$$

This strength was adopted in limit equilibrium analyses for the short length of the failure surface passing through the zone I fill. In FE analyses the strengths mobilized at failure were well beyond peak, and for simplicity the strengths were assumed to be the same as those for the type II fill.

STABILITY ANALYSIS

Analysis of the initial slip

A representative section at ch. 725 was analysed (Fig. 23). Crest level at failure was el. 201. Vaughan (1991) has shown that a deep-seated slide in brittle soil fails without three-dimensional effects if longer than a critical length. The length of the initial failure was greater than the critical length, and the section could be analysed in two dimensions without error.

Limit equilibrium analysis. Stability was investigated using a multiple wedge analysis incorporating six vertical slices, with, typically, interslice forces acting at an angle $\delta = 10°$. This gave closely similar results to analyses using the simplified assumptions of Morgenstern & Price (1965). Pore pressures in the core and boot were taken from the mean line of Fig. 9. The Yellow Clay must have been fully consolidated, with ground water level at the base of the layer just before failure, and zero pore pressure was assumed. A strength of $c' = 0$, $\Phi' = 30°$ was adopted for the short length of the slip through the slope protection and berm fill. This assumption has little influence on the results of the analysis. Various slip surfaces were tried through the core, within the bounds shown in Fig. 23. The

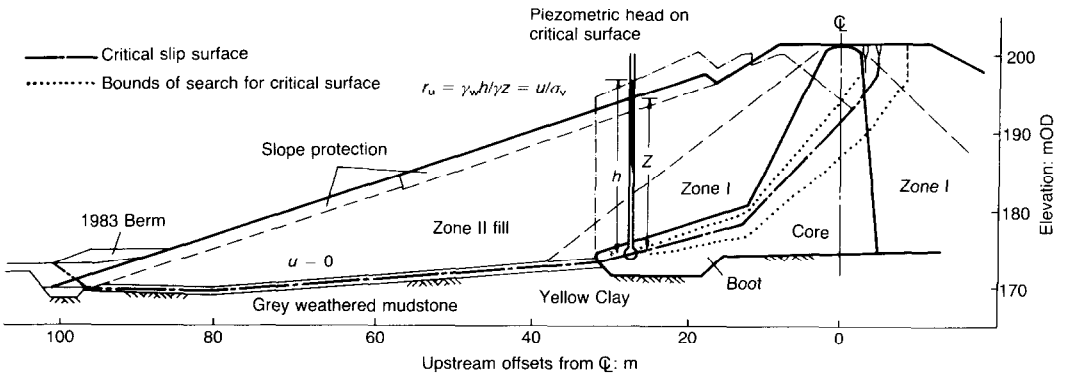

Fig. 23. Initial failure ch. 725: limit equilibrium stability analysis (unit weights (kN/m³): core and boot 18·5, zone I 20·5, zone II 22·0 slope protection 18·5; average values of τ_u 0·42 in core, 0·53 in boot)

surface that gives the lowest factor of safety is almost coincident with the actual one.

The results of the analysis are given in Table 3. If the measured intact strengths are adopted, the safety factor is $F_1 = 1{\cdot}41$. This reduces by 14% to $F_2 = 1{\cdot}21$ if the strengths are reduced to allow for solifluction shears in the Yellow Clay and rutting shears in the core. A further reduction of 17% is required to account for failure ($F_3 = 1$). This reduction can be attributed to progressive failure.

From the FE analysis that reproduces the failure height, the average shear strain along the eventual slip surface through the core just before failure is about 12%, and the laboratory triaxial tests, after correction for the presence of random shears, give a mobilized strength at this strain of $c' = 1{\cdot}5$ kPa, $\Phi' = 19°$. When this strength is assumed for the core the average strength of the Yellow Clay at failure becomes $c' = 0$, $\Phi' = 16°$, about halfway between peak (allowing for shears) and residual. This is lower than the strength approximately equivalent to critical state ($c' = 0$, $\Phi' = \Phi_p'$), an assumption often made on empirical grounds as safe for the strength of plastic clays.

The values of safety factor given in Table 3 cannot be considered precise, but there is little scope for variations in F_1 as the slip geometry, pore pressures, unit weights and intact peak strengths are known within narrow margins. The uncertainty in the method of analysis (examined by varying δ between reasonable limits) does not exceed about 5%. However, there is some uncertainty regarding the extent and contribution of the solifluction shears in the Yellow Clay. The assumption that 40% was sheared, used in calculating F_2, is the average from the field observations in the vicinity of the slip, but there were quite large variations between the different pits examined. A figure of 50%, the average for the whole site, was adopted in an early analysis (Skempton, 1985). This is a reasonable upper limit for the area of the slip. 20% is about the smallest proportion found in any one test pit, and is a reasonable lower bound. Table 4 gives values of F_2 at these limits. The reductions remaining to be attributed to progressive failure are 14% and 21% respectively. These figures indicate that solifluction shears could not have accounted for the slip without the additional effect of progressive failure. Conversely, it is unlikely that the influence

Table 3. Limit equilibrium analysis: initial failure ch. 725 (crest level el. 201)

Condition	Core		Yellow Clay		Factor of safety	Reduction: %	Combined reduction: %
	c: kPa	Φ'	c: kPa	Φ'			
Peak, intact	15	21°	10	20°	$F_1 = 1{\cdot}41$		
Peak, with shears	6	20°	6	18°	$F_2 = 1{\cdot}21$	$\frac{F_1 - F_2}{F_1} = 14$	
At failure	1·5	19°	0	16°	$F_3 = 1{\cdot}00$	$\frac{F_2 - F_3}{F_2} = 17$	$\frac{F_1 - F_3}{F_1} = 29$
Residual	0	13°	0	12°	$F_R = 0{\cdot}71$		

Table 4. Parametric study of stability: initial failure ch. 725

F_1 (peak, intact)	1·41		
F_3 (at collapse)	1·00		
Proportion of Yellow Clay with shears	20%	40%	50%
Resultant strength	$c_p' = 8$ kPa $\Phi_p' = 19°$	$c_p' = 6$ kPa $\Phi_p' = 18°$	$c_p' = 5$ kPa $\Phi_p' = 17·5°$
F_2 (peak with shears)	1·27	1·21	1·17
Reduction factors due to			
shears $(F_1 - F_2)/F_3$	10%	14%	17%
progressive failure $(F_2 - F_3)/F_2$	21%	17%	14%

of progressive failure alone could have been sufficient to account for failure without some effect from solifluction shears.

Finite element analysis. An FE analysis of the initial slip using a strain softening elasto-plastic soil model incorporating the material strengths described by Potts *et al.* (1990) reproduced peg movements, pre-failure settlements, pore pressures in the core and the height at failure that agree well with those observed. It also recovered the observed slip surface for the inner part of the slip which formed before failure. The analysis cannot reproduce the formation of the outer part of the slip surface which formed after failure, as the embankment is then no longer in equilibrium. The analysis assumed a strength in the Yellow Clay equivalent to 40% shears, and an undrained strength in the core and boot equivalent to the effective stress assumptions used in the limit equilibrium analysis to derive F_2.

Figure 24, derived from this analysis, shows how progressive failure reduced the average strength available. The highly non-uniform strains along the Yellow Clay vary from 30% near the boot to 5% near the toe, and they also vary in the core and boot. Just before failure part of the Yellow Clay had been strained well past peak strength, and part had not reached peak. Thus the average shearing resistance available was much less than peak. The degree of progressive failure is determined directly in these analyses, and can be expressed in terms of the residual factor R for each material, with $R = (\tau_p - \tau_m)/(\tau_p - \tau_R)$, where τ_m, τ_p and τ_R are the average mobilized, peak and residual strengths respectively. In the Yellow Clay, $R = 0·52$ was predicted. In the core and boot nearly all the fill had exceeded peak, and $R = 0·42$. These strength losses are closely equivalent to those that must be assumed in the limit equilibrium analysis to account for failure.

The strains predicted by the FE analysis in the

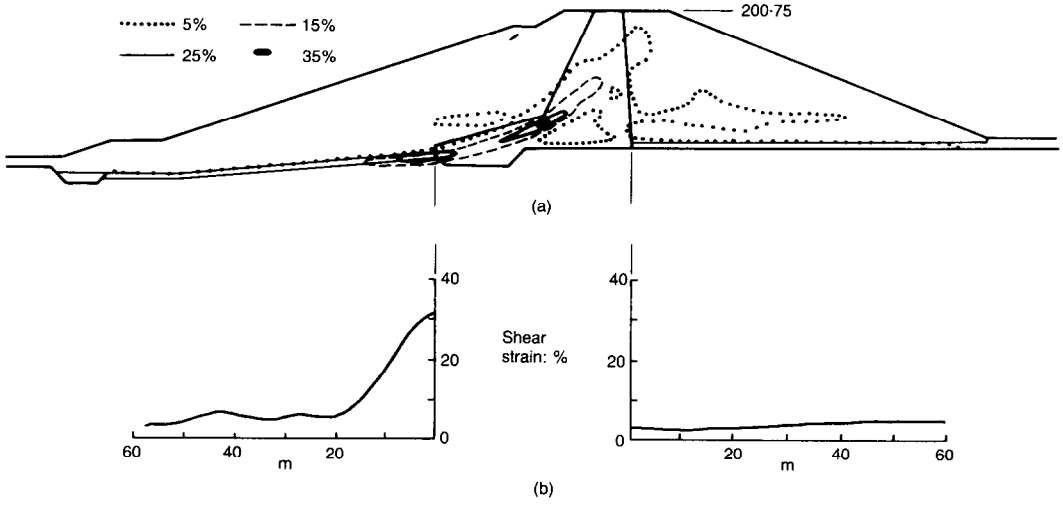

Fig. 24. Initial failure ch. 725—strains predicted by FE analysis just before collapse: (a) contours of deviatoric strain; (b) shear strain distribution along Yellow Clay

Yellow Clay below the downstream slope are also shown in Fig. 24. They are small and all the clay is some way from failure: this is consistent with the stability of this slope, although it was steeper than the one that failed. The strains at this point are also relatively uniform. Dounias *et al.* (1989) have considered what would have happened had the thrust from the core become sufficient to load the downstream side more severely.

Analysis of the failure in the valley centre

Three-quarters of the length of the slide did not fail initially; it failed only after significant movement had occurred at the initial failure. It was difficult to assume that the whole length of the slide had a safety factor of one on 4 June, since it varied in height from 17 m to 37 m, and different lengths passed through different materials. It was concluded that most of the slide was dragged to failure by the initial movement (Vaughan, 1985, 1991), in the following manner.

Once the initial section starts moving, the strength on the whole of the slip surface falls to residual, and the slip mass is not in equilibrium unless it is acted on by a restraining force, exerted by the as yet unfailed embankment on either side. The force transferred to the next lengths of embankment cause these to fail in turn. The new lengths then exert similar forces on the next lengths, which fail in turn, and so on. This domino effect may lead to lateral propagation of the slip (as witnessed on 4–6 June) even when the slope outside the initial failure had a safety factor greater than one.

Vaughan (1985, 1991) has shown that, for the Carsington slope, this effect would be halted only if the safety factor of the next unfailed section was greater than $\sim 1{\cdot}3$ (by an analysis giving $F = 1$ for the initial failure). At such a point an end shear would form. He also deduced that load transfer would not operate around a convex curve in the slope, as sections would then separate during sliding. The slide stopped at its north end almost exactly at the tangent point to the curve in the dam axis (Fig. 2).

If lateral load transfer is operating during a failure, then the factor of safety, as conventionally defined by two-dimensional analysis, can be greater than one. This was probably true in the valley centre at Carsington, and thus back-analysis of the slip could not be used to determine the average strength of the materials involved, as was done for the initial failure. Nonetheless, analysis of this part of the slide is valuable, to ensure that a satisfactory explanation of the whole event has been established.

Limit equilibrium analysis. A composite section equivalent to that at ch. 850 was analysed. The observations of the slip surface made during removal of the dam (Fig. 17) showed that this section was representative of a considerable length of bank where failure had occurred through the base of the fill. The method of analysis used was as for the initial failure, with pore pressures in the core and boot from Fig. 9, and pore pressures in the mudstone fill given by the measured ground water level at el. 170. Factors of safety were derived (Tables 5 and 6) for the best estimates of strength described above. With peak intact strengths, $F_1 = 1{\cdot}60$. These strengths were then reduced to allow for rutting shears in the core (as for the initial failure) and by varying amounts to allow for layered structure in the mudstone fill. With a peak strength in zone II fill of $c_p' = 13{\cdot}5$ kPa, $\Phi_p' = 24°$, equivalent to a reduction of 20% from peak to residual (or 10% reduction of peak intact strength), $F_2 = 1{\cdot}44$. For 10% and 40% reduction from peak to residual, corresponding respectively to 5% and 20% reduction of peak strength, $F_2 = 1{\cdot}48$ or $1{\cdot}34$ (Table 6). As is shown below, these are extreme cases, and they imply reductions in factor of safety due to pre-existing shears in the core and boot and layered structure in the mudstone fill between the limits 8% and 16%.

If lateral load transfer is operating during a failure, the factor of safety as conventionally

Table 5. Limit equilibrium analysis: valley centre ch. 850 (crest level el. 200)

Condition	Core		Zone I		Zone II		Factor of safety
	c_p': kPa	Φ_p'	c_p': kPa	Φ_p'	c_p': kPa	Φ_p'	
Peak, intact	15	21°	10	22°	17	26°	$F_1 = 1{\cdot}60$
Peak, with structure*	6	20°	10	22°	13·5	24°	$F_2 = 1{\cdot}44$
Before load transfer†	0	19°	0	19·6	0	19·6	$F_3 = 1{\cdot}09$
At failure							$F_4 = 1{\cdot}00$
Residual	0	13°	0	14°	0	15°	$F_R = 0{\cdot}77$

* Rutting shears in core and boot, 10% strength reduction in strength of zone II fill.

† Equivalent to failure without load transfer at crest level el. 203.

Table 6. Parametric study of stability: valley centre ch. 850

F_1 (peak, intact)	1·60		
F_4 (failure at el. 200 with load transfer)	1·00		
Strength reduction in zone II from peak: % From peak to residual: %	5 10	10 20	20 40
Strength c_p': kPa Zone II fill Φ'	15 24°	13·5 24°	10 22°
F_2 (peak with shears)	1·48	1·44	1·34
Failure level (no load transfer): $el._f$	205, 204, 203	204, 203, 202	202, 201, 200
F_3 (crest at el. 200) (no load transfer)	1·15, 1·12, 1·09	1·12, 1·09, 1·06	1·06, 1·03, 1·00
Reduction factors For strength reduction $(F_1 - F_2)/F_1$: % For progressive failure $(F_2 - F_3)/F_2$: % For load transfer $(F_3 - F_4)/F_3$: %	 8 22, 24, 26 13, 11, 8	 10 22, 24, 26 11, 8, 6	 16 21, 23, 25 6, 3, 0

defined by two-dimensional analysis will be greater than 1·0. Thus the true factor of safety at the actual crest elevation before load transfer affected the valley centre section F_3 is greater than 1·0. Direct back-analysis, as was done for the initial failure, is not possible. Nonetheless, analysis of this part of the slide can be carried out by combining limit equilibrium and FE analyses, and is valuable in ensuring that a satisfactory explanation of the whole event has been established.

The problem can be solved if the height to which the valley centre section could be built without load transfer, defined as the failure crest level $el._f$, is determined. Irrespective of any calculations, field evidence for peg displacements and other observations before failure strongly suggest that, even without load transfer, the bank could not have been raised much above its crest level of el. 200 at the time of collapse. As a reasonable assumption (later to be justified by FE analysis), the failure crest level could be taken at $el._f = 203$. A two-dimensional back-analysis can then be made, since at this crest level (with no load transfer) $F = 1·00$. This gives $c' = 0$ and $\Phi' = 19·6°$ in the mudstone fill, adopting $c' = 0$, $\Phi' = 19°$ in the core and boot, a slightly lower strength than at ch. 725 compatible with larger strains in the deeper section at ch. 850. These parameters can then be used to calculate the factor of safety of the bank at its actual crest level of el. 200, before load transfer. This gives $F_3 = 1·09$.

If failure crest level $el._f = 200$, then by definition $F_3 = 1·00$. Thus the value of F_3 for any other failure crest level can be found by interpolation, e.g. for $el._f = 201$, $F_3 = 1·03$.

Finite element analysis. Dounias (1987) has given details of an analysis of the valley centre section at ch. 850 using a peak strength equivalent to $c_p' = 13·5$ kPa, $\Phi_p' = 24°$ for the zone II fill, with other material properties as described above and an allowance for rutting shears in the core and boot as at ch. 725. It predicts a failure crest level at el. 201 and recovers the observed behaviour in terms of pore pressure and setttlement. However, the horizontal movements were generally overestimated (see Fig. 11) and it was thought that the horizontal stiffness of the mudstone fill had been underestimated. This would lead to too much progressive failure in the analysis. When this effect was taken into account, a failure crest level of $el._f = 202$ was estimated. Parametric studies indicated that varying assumptions for stiffness and rate of strain softening between reasonable bounds changed the failure crest level by ± 1 m.

A similar analysis based on $c_p' = 15$ kPa, $\Phi_p' = 25°$ in zone II fill (corresponding to a 5% reduction from intact peak strengths, or 10% reduction from peak to residual) gave a failure crest level at $el._f = 203$; which again could be increased by 1 m to $el._f = 204$ with greater horizontal stiffness of the mudstone fill. By linear extrapolation, the predicted failure crest level for $c_p' = 10$ kPa and $\Phi_p' = 22°$ in zone II fill (corresponding to a 20% reduction from intact peak strengths or 40% from peak to residual), is $el._f = 201$.

Reconciliation of limit equilibrium and finite element analyses

For a given set of (reduced) peak strength parameters a rational solution to the problem of analysing the valley centre section can be

obtained. Taking $c_p' = 13{\cdot}5$ kPa, and $\Phi_p' = 24°$ in zone II fill, the steps are as follows.

(*a*) By limit equilibrium analysis, the factor of safety at the actual crest level el. 200, before load transfer and without progressive failure, is 1·44.
(*b*) By FE analysis, the failure crest level with no load transfer but allowing for progressive failure is $el._f = 203$.
(*c*) Back-analysis then gives strength parameters corresponding to $F = 1{\cdot}0$ at el. 203.
(*d*) From (*c*), the factor of safety at the actual crest level el. 200, before load transfer, can be found: $F_3 = 1{\cdot}09$.
(*e*) The reductions in factors of safety are then: 10% due to pre-existing shears and layered structure (from $F_1 = 1{\cdot}60$ to $F_2 = 1{\cdot}44$), 24% due to progressive failure (from $F_2 = 1{\cdot}44$ to $F_3 = 1{\cdot}09$) and 8% due to load transfer (from $F_3 = 1{\cdot}09$ to $F_4 = 1{\cdot}00$).

The results of exactly similar calculations allowing for an uncertainty of ± 1 m in the failure crest level predicted by the FE analysis are given in Table 6 for this case and also for peak strengths of zone II fill reduced by 5% and 20% below the intact value. They cover the entire range of possible solutions, from a failure crest level at el. 200 (the extreme lower limit) to el. 205, which from field observation is almost certainly an extreme upper limit.

From Table 6 it is apparent that, over this wide range, the reduction in factor of safety due to progressive failure varies only from 21% to 26%. Over the more probable range of $el._f$ from el. 201 to el. 204 there is scarcely any variation, the reduction being 23% or 24%. Thus the effect of progressive failure in the valley centre section was decidedly more than in the initial slip. This is compatible with a degree of non-uniformity of strain along the potential slip surface near the base of the mudstone fill at ch. 850, as shown by FE analysis, substantially greater than in the Yellow clay at ch. 725. The most probable results for the valley centre section and the initial slip are summarized in Table 7.

Table 7. Summary of reductions in safety factor at the initial failure and in the valley centre

Effect	Reduction in safety factor: %	
	Initial failure ch. 725	Valley centre ch. 850
Pre-existing structure*	14	10
Progressive failure	17	24
Load transfer	0	8

* Including shears and layered structure in the mudstone fill.

Table 8. Factors of safety at other sections: failure through core, boot and Yellow Clay

Chainage : m	Factor of safety
600	1·06
650	1·02
675	1·02
700	1·06
725*	1·00*
750	1·05
775	1·17
1000	1·11
1025	1·17
1050	1·18

* Minimum at initial failure.

Analyses of other sections

A positive demonstration of the presence of lateral load transfer is obtained through analysis of other sections on the valley sides (Vaughan, 1991). At these sections the failure was through common materials (the core and the Yellow Clay), the only difference between sections being in geometry. Safety factors deduced from limit equilibrium analysis on the assumption that $F = 1$ at the initial failure are given in Table 8. It can be seen that factors of safety elsewhere are substantially greater than one. Failure of these other sections can be explained only by lateral load transfer. Vaughan (1991) has also examined the stability of different sections of the slide after it came to rest, and has shown that lateral load transfer must still have been operating.

FINAL COMMENTS

The initial failure could be analysed in two dimensions without error. The factor of safety of 1·4, based on limit equilibrium analyses using peak intact strengths, was rather low by conventional standards, particularly for a deep-seated movement. This arose due to the wide boot of weak undrained clay. Pre-existing shears lowered the safety factor to about 1·2; progressive failure reduced the average strength further, and led to collapse.

While movements prior to collapse were sufficiently large to cause concern, the measured deformation did not accelerate to indicate imminent failure until just before collapse. This suggests that, when progressive failure is involved, measurements of deformation cannot be relied on for monitoring stability.

The initial failure, which was about 100 m long, spread by lateral load transfer through other sections of the slope with factors of safety greater than one, until the final length of the slip was nearly 500 m.

The highest section in the valley centre, in which failure occurred in the fill rather than in the foundation, failed due to lateral load transfer, with a safety factor prior to collapse of the order of 1·1. The safety factor predicted using intact strengths was about 1·6, and with allowance for strength reductions it was about 1·4. The reduction to $F = 1{\cdot}1$ was due to progressive failure, which had a greater influence here than at the initial failure.

To allow for uncertainties in the strength of plastic clays and similar materials, an empirical reduction is often adopted in limit equilibrium analysis by assuming $c' = 0$. At Carsington this assumption gives safety factors of the order of 1·2–1·3, and is insufficient to predict collapse.

The large effect of progressive failure found at Carsington is probably due to a combination of the boot, which makes deep-seated movement the critical mode of collapse, and to the sharp discontinuity of shearing resistance at the boot/yellow clay boundary, which promotes non-uniform strain. This large effect may not be typical, and the adoption of a general empirical factor to allow for it could be unnecessarily conservative. The risk of progressive failure can be examined by numerical analysis.

ACKNOWLEDGEMENTS

The Authors gratefully acknowledge the permission of Severn Trent plc to publish this Paper. They thank Babtie Shaw & Morton for their joint contribution to the work described and for assistance in preparation of the Paper. Many others who also contributed are also thanked.

NOTATION

c_p', Φ_p'	peak strength
c_{ps}', Φ_{ps}'	average peak drained strength
c_r', Φ_r'	drained residual strength
c_s', Φ_s',	residual shearing resistance on surface
i	angle of dilation
q^*	bulk strength of mass of soil
q_p	shear strength at failure of intact soil
R	residual factor
W_L	liquid limit
W_p	plastic limit
w	water content
δ	angle of interslice forces
ξ	equation (3) parameter
τ_m, τ_p, τ_R	average mobilized, peak and residual strengths

REFERENCES

Coxon, R. E. (1986). *Failure of Carsington Embankment.* Report to the Secretary of State for the Environment. London. HMSO.

Dounias, G. T. (1987). *Progressive failure in embankment dams.* PhD thesis, University of London.

Dounias, G. T., Potts, D. M. & Vaughan, P. R. (1988). The shear strength of soils containing undulating shear zones: a numerical study. *Can. Geotech. J.* **25,** 550–558.

Dounias, G. T., Potts, D. M. & Vaughan, P. R. (1989). *Numerical stress analysis of progressive failure and cracking in embankment dams.* Report to the Department of the Environment, Contract PECD 7/7/222. Garston: Building Research Establishment.

Morgenstern, N. & Price, V. E. (1965). The analysis of the stability of general slip surfaces. *Géotechnique* **15,** No. 1, 79–93.

Penman, A. D. M. (1986). On the embankment dam. *Géotechnique* **36,** No. 3, 301–347.

Potts, D. M., Dounias, G. T. & Vaughan, P. R. (1990). Finite element analysis of progressive failure of Carsington embankment. *Géotechnique* **40,** No. 1, 79–101.

Rocke, G. (1993). Investigation of the failure of Carsington Dam. *Géotechnique* **43,** No. 1, 175–180.

Sandroni, S. S. (1976). *Total and effective stress strength behaviour of London clay.* PhD thesis, University of London.

Skempton, A. W. (1985). Geotechnical aspects of the Carsington Dam failure. *Proc. 11th Int. Conf. Soil Mech.*, San Francisco **5,** 2581–2591.

Skempton, A. W. & Coats, D. J. (1985). Carsington Dam failure. *Failure in earthworks,* pp. 203–220. London: Thomas Telford.

Vaughan, P. R. (1985). Discussion on questions raised by the Carsington Dam slide. Influence of random discontinuities on shear strength, and lateral load transfer. *Proc. 11th Int. Conf. Soil Mech., San Francisco* **5,** 2817–2818.

Vaughan, P. R. (1991). Stability analysis of deep slides in brittle soil—lessons from Carsington. *Slope Stability Engineering.* pp. 1–11. London: Thomas Telford.

Vaughan, P. R. & Chalmers, R. W. (1992). Discussion on A reassessment of the Carsington embankment failure by P. W. Rowe. *Géotechnique* **42,** No. 3, 517–521.

White, I. L. & Vakalis, I. G. (1983). An investigation into the development of polished interfaces in clay fills. *Proc. 8th Eur. Conf. on Soil Mech., Helsinki* **1,** 323–326.

White, I. L. & Vakalis, I. G. (1985). Smooth slip surfaces in clay fills resulting from soil machine interaction. *Failure in Earthworks,* pp. 445–447. London: Thomas Telford.

White, I. L. & Vakalis, I. G. (1987). Shear surfaces induced in clay fills by compaction plant. *Compaction technology,* pp. 125–138. London: Thomas Telford.

BIBLIOGRAPHY

Kennard, M. F. (1985). Discussion *Failure in earthworks,* pp. 233–235. London: Thomas Telford.

Rowe, P. W. (1985). The potentially latent dominance of groundwater in ground engineering. *Ground water in engineering,* Engineering Geology Special Publication No. 3, pp. 27–43. London: Geological Society.

Rowe, P. W. (1991). A reassessment of the Carsington embankment failure. *Géotechnique* **41,** No. 3, 395–422.

Skempton, A. W., Norbury, D., Petley, D. J. & Spink, T. W. (1988). Solifluction shears at Carsington, Derbyshire. *Quaternary Engineering Geology*, Engineering Geology Special Publication No. 7, pp. 381–387. London: Geological Society.

Skempton, A. W. & Vaughan, P. R. (1989). Discussion on the predictability of the failure at Carsington. *Clay barriers for embankment dams*, pp. 182–186. London: Thomas Telford.

Vaughan, P. R. (1989). Discussion on An examination of the possibility of detecting the Carsington dam failure in advance through instrumentation. *Instrumentation in civil engineering projects*, pp. 458–462. London: Thomas Telford.

Vaughan, P. R., Dounias, G. T. & Potts, D. M. (1989). Advances in analytical techniques and the influence of core geometry on behaviour. *Clay Barriers for embankment dams*, pp. 87–108. London: Thomas Telford.